Soft gluon resummation for gluon fusion *ZH* production

Goutam Das,[1,*] Chinmoy Dey,[2,†] M. C. Kumar,[2,‡] and Kajal Samanta[3,§]

[1]*Institut für Theoretische Teilchenphysik und Kosmologie, RWTH Aachen University, D-52056 Aachen, Germany*

[2]*Department of Physics, Indian Institute of Technology Guwahati, Guwahati-781039, Assam, India*

[3]*Institute for Particle Physics Phenomenology, Durham University, Durham DH1 3LE, United Kingdom*

(Received 25 February 2025; accepted 5 January 2026; published 23 January 2026)

We examine the effects of soft gluons on Higgs boson production in association with a Z boson at the Large Hadron Collider (LHC). Utilizing the universal cusp anomalous dimensions and splitting kernels, we analyze effects of soft gluons on the gluon fusion ZH process, focusing on the total production cross section as well as the invariant mass distribution at the next-to-leading logarithmic level. Additionally, we estimate the next-to-soft effects on this subprocess to the same level of accuracy. A detailed phenomenological analysis is performed for the 13.6 TeV LHC. Finally, combining these results with those from other subprocesses, we provide comprehensive predictions for the ZH production cross section and the invariant mass distribution that will be valuable for comparison with experimental data from the upcoming LHC run as well as the future hadron colliders.

DOI: 10.1103/mxxw-bvm3

I. INTRODUCTION

The discovery of the Higgs boson [1–3] at the Large Hadron Collider (LHC) [4,5] marks a significant milestone in particle physics. Following this breakthrough, the primary focus of the LHC has been the precise measurement of the Higgs boson's properties and couplings. Such efforts not only deepen our understanding of the Higgs boson itself but also open new avenues for exploring physics beyond the standard model (BSM). Many BSM scenarios predict weak couplings to the Higgs boson at collider energies in the TeV range. Evidence of such interactions may manifest as deviations in total cross sections or distributions for Higgs boson processes. Therefore, precise experimental measurements, combined with accurate theoretical predictions, are critical for identifying potential BSM signatures. The associated Higgs production with a vector boson at the LHC is of particular importance in probing Higgs coupling to the weak gauge bosons. Furthermore, it is crucial to constrain the sign of the top-quark Yukawa coupling and examine its CP structure [6–8]. Keeping in mind the importance of this process, the ATLAS and CMS experiments are actively conducting precise measurements for this process [9–19]. Precise theoretical predictions are thus essential to complement the improved experimental results for this channel.

At the LHC, the Higgs boson is produced in association with Z boson primarily through the Drell-Yan (DY) type subprocess ($q\bar{q} \to Z^* \to ZH$) at the leading order (LO) in the strong coupling (α_s) expansion. The higher-order quantum chromodynamics (QCD) corrections for this channel thus closely follow the DY process and have been computed up to next-to-next-to-leading order (N2LO) [20–27] and recently to next-to-next-to-next-to-leading order (N3LO) [28] accuracy. The perturbative series for the DY-type contribution converges very quickly with next-to-leading order (NLO), amounting to around 30% correction to LO, whereas N2LO and N3LO receive around 3% and −0.8% corrections, respectively, relative to preceding orders. Additionally, the conventional theoretical scale uncertainty reduces to subpercent level. The ZH process also gets a contribution from the bottom quark annihilation through the t-channel diagrams at the LHC. This involves a bottom Yukawa coupling (y_b), and its contribution is found [29] to be at the subpercent level. Furthermore, the electroweak effects for this DY-type process have been computed to NLO [30] and a correction of around −5% was observed compared to the NLO QCD result. When fiducial cuts are applied, these corrections can grow significantly, reaching −10% to −20% of the NLO QCD distributions [31].

Compared to the DY process, the ZH production process receives additional QCD contributions starting from N2LO.

*Contact author: goutam@physik.rwth-aachen.de
†Contact author: d.chinmoy@iitg.ac.in
‡Contact author: mckumar@iitg.ac.in
§Contact author: kajal.samanta@durham.ac.uk

Published by the American Physical Society under the terms of the Creative Commons Attribution 4.0 International license. Further distribution of this work must maintain attribution to the author(s) and the published article's title, journal citation, and DOI. Funded by SCOAP³.

One such contribution arises from Feynman diagrams in which the Higgs boson is radiated off a massive top-quark loop in the quark-antiquark annihilation subprocess. The impact of this contribution has been estimated in [32] to be below 3%.

Another class of subprocesses that first appears at N2LO, i.e., at $\mathcal{O}(\alpha_s^2)$, is the gluon fusion channel for ZH production. Although the gluon fusion subprocess is suppressed by two powers of the strong coupling constant compared to the quark-antiquark annihilation channel, this suppression is largely compensated by the sizable gluon luminosity at the LHC. Consequently, from N2LO onwards, the gluon fusion contribution becomes phenomenologically significant. Due to its importance, the gluon fusion subprocess has been extensively investigated in the literature. At leading order [which contributes at $\mathcal{O}(\alpha_s^2)$], it is a loop-induced process in which the ZH final state is produced via massive quark loops comprising both triangle and box topologies (see Fig. 2 of [33]), with the top quark providing the dominant contribution. The gluon fusion subprocess at LO has been shown [33–36] to yield a correction of about 7% relative to the NLO QCD DY-type contribution. In contrast, the N2LO QCD DY-type correction amounts to only about 3% relative to NLO DY. The scale uncertainty of the gluon fusion contribution at leading order is approximately 25%.

Several efforts have been made to further improve the accuracy of the gluon-initiated subprocess by calculating its NLO [$\mathcal{O}(\alpha_s^3)$] contribution. This calculation involves two-loop amplitudes with multiple kinematic scales, including three masses: the Higgs boson mass (M_H), the Z boson mass (M_Z), and the top-quark mass (m_t), as well as two Mandelstam variables. The presence of such a large number of scales substantially increases the computational complexity. The problem, however, becomes considerably simpler in the infinite top-mass [effective field theory (EFT)] limit, where the NLO correction has been computed 37]]. Nevertheless, ongoing efforts aim to account for the full top-mass dependence. The NLO real and virtual contributions have been evaluated using an asymptotic expansion in the inverse top-quark mass [38]. In addition, two-loop amplitudes have been computed through high-energy and large-m_t expansions employing the Padé approximation [39], as well as through a transverse-momentum expansion [40]. The combined effects of the high-energy and transverse-momentum expansions have been further investigated in Refs. [41,42]. The NLO cross section and invariant mass distribution have also been computed by incorporating the full top-quark mass dependence, supplemented by a small-mass expansion in M_H and M_Z [43]. More recently, two-loop virtual corrections including full top-mass effects have been evaluated [44], followed by a determination of the NLO cross section with complete top-mass dependence [45]. The resulting NLO total cross section is found to increase by approximately 100% relative to the leading-order prediction, while the associated scale uncertainty is reduced to about 15%. In contrast, differential distributions, such as the Higgs boson transverse-momentum spectrum within the fiducial phase space, can receive corrections as large as an order of magnitude.

The fixed-order results for this subprocess still suffer from the large threshold logarithms arising from soft gluons' emission. These large logarithms need to be resummed to have reliable predictions. The size of the NLO corrections indicates that this subprocess will receive significant contributions from the threshold logarithms, similar to the Higgs case. Resummation of these large soft-virtual (SV) logarithms is well established in the literature [46–58] and they have been applied to many colorless processes [59–77], leading to improved predictions for inclusive cross sections and invariant mass distributions. Recently, efforts were made to incorporate also the next-to-soft (NSV) threshold effects [78–98].

For the ZH production in the DY-type channel, the effects of soft gluons have been estimated in [99–101] to next-to-next-to-next-to-leading logarithmic (N3LL) accuracy matched to N3LO fixed order in QCD. A better perturbative convergence has been observed for threshold resummation for invariant mass distribution of ZH pair. For the gluon fusion ZH process, the impact of soft gluon effects on the total cross section has been investigated in [102] to next-to-leading logarithmic (NLL) accuracy matched to NLO in the EFT approximation using two different threshold definitions, namely, the M approach and the Q approach. In the M approach, the threshold is defined in terms of the total mass of the ZH system, while in the Q approach, it is defined using the invariant mass of the ZH system. Although both approaches yield results that are consistent within the scale uncertainties, the Q approach exhibits better perturbative stability and slightly reduced scale dependence.

The goal of this paper is to improve the gluon fusion ZH process by incorporating soft and next-to-soft gluon resummation for both the total cross section and the invariant mass distribution of the ZH pair. We work in the exact Born-improved gluon fusion channel, which has been shown to work effectively for the Higgs case, and we expect similar behavior for the ZH process. For NSV resummation, we closely follow the approach outlined in [91,92]. Additionally, we present the complete result at $\mathcal{O}(\alpha_s^3)$, improved with SV threshold resummation from both quark and gluon channels for ZH production.

The article is organized as follows: in Sec. II, we introduce the key theoretical formulas and present the coefficients required for performing SV and NSV resummation up to the necessary order. In Sec. III, we provide a phenomenological study for the gluon fusion subprocess, combining it with the DY-type contributions to present complete results for pp collisions at $\mathcal{O}(\alpha_s^3)$ accuracy. Finally, we conclude in Sec. IV.

II. THEORETICAL FRAMEWORK

The hadronic cross section for ZH production in proton collision is provided in QCD factorization as

$$Q^2\frac{\mathrm{d}\sigma}{\mathrm{d}Q^2}=\sum_{a,b}\int_0^1\mathrm{d}x_1\int_0^1\mathrm{d}x_2 f_a(x_1,\mu_F^2)f_b(x_2,\mu_F^2)\times\int_0^1\mathrm{d}z\,\delta(\tau-zx_1x_2)Q^2\frac{\mathrm{d}\hat{\sigma}_{ab}(z,\mu_F^2)}{\mathrm{d}Q^2},\tag{2.1}$$

where $f_{a,b}$ are the parton distribution functions (PDFs) for parton a, b in the incoming hadrons and $\hat{\sigma}_{ab}$ is the partonic coefficient function. The hadronic and partonic threshold variables $\tau=Q^2/S$ and $z=Q^2/\hat{s}$ are defined in terms of respective center-of-mass energies S and $\hat{s}$. Here, Q is the invariant mass of the ZH system and μ_F is the factorization scale. The partonic coefficient function can be decomposed (suppressing all scale dependencies) as

$$Q^2\frac{\mathrm{d}\hat{\sigma}_{ab}(z)}{\mathrm{d}Q^2}=\hat{\sigma}_{ab}^{(0)}(Q^2)(\delta_{ba}\Delta_{ab}^{\mathrm{SV}}(z)+\Delta_{ab}^{\mathrm{REG}}(z)).\tag{2.2}$$

The term $\Delta_{ab}^{\mathrm{SV}}$ appears only for the diagonal subprocesses (gg, $q\bar{q}$) and is known as the soft-virtual partonic coefficient and it captures the leading singular terms in the $z\equiv 1-\bar{z}\to 1$ limit. The $\Delta_{ab}^{\mathrm{REG}}$ term, on the other hand, contains subleading or regular contributions in the variable z. In general, they follow the expansion in the strong coupling at the renormalization scale $\alpha_s(\mu_R^2)\equiv 4\pi a_s(\mu_R^2)$ as

$$\begin{aligned}\Delta_{ab}^{\mathrm{SV}}(z)&=\sum_{n=0}^{\infty}a_s^n(\mu_R^2)\delta_{ab}\left(\Delta_\delta^{(n)}\delta(\bar{z})+\sum_{k=0}^{2n-1}\Delta_{\mathcal{D}_k}^{(n)}\mathcal{D}_k(\bar{z})\right),\quad\text{with}\quad ab\in\{gg,q\bar{q}\},\\ \Delta_{ab}^{\mathrm{REG}}(z)&=\Delta_{ab}^{\mathrm{NSV}}(z)+\sum_{n=0}^{\infty}a_s^n(\mu_R^2)\Delta_{ab}^{(n)}(z)=\sum_{n=0}^{\infty}a_s^n(\mu_R^2)\left(\sum_{k=0}^{2n-1}\Delta_{ab,\ln_k}^{(n)}\ln^k(\bar{z})+\Delta_{ab}^{(n)}(z)\right),\end{aligned}\tag{2.3}$$

where $\delta(\bar{z})$ is the Dirac delta distribution and $\mathcal{D}_k(\bar{z})\equiv[\ln^k(\bar{z})/\bar{z}]_+$ are the plus distributions. At leading order, all the coefficients vanish except $\Delta_\delta^{(0)}=1$. Here, $\Delta_{ab,\ln_k}^{(n)}$ are the NSV coefficients, which get contributions from both diagonal as well as off-diagonal channels. The last term in the above expression $\Delta_{ab}^{(n)}(z)$ vanishes in the soft limit $\bar{z}\equiv 1-z\to 0$. Note that the singular SV part of the partonic coefficient has a universal structure, which gets contributions from the underlying hard form factor, mass factorization kernels [103,104], and soft radiations [54,55,105–108]. All of these are infrared divergent, which, however, when regularized and combined give finite contributions.

The Born normalization factor $\hat{\sigma}_{ab}^{(0)}$ in Eq. (2.2) takes the following form for the $q\bar{q}$ subprocess:

$$\hat{\sigma}_{q\bar{q}}^{(0)}(Q^2)=\left(\frac{\pi\alpha^2}{n_cS}\right)\left[\frac{M_Z^2\lambda^{1/2}(Q^2,M_H^2,M_Z^2)\left(1+\frac{\lambda(Q^2,M_H^2,M_Z^2)}{12M_Z^2/Q^2}\right)}{(Q^2-M_Z^2)^2c_w^4s_w^4}((g_q^V)^2+(g_q^A)^2)\right],\tag{2.4}$$

with $g_a^A=-\frac{1}{2}T_a^3$, $g_a^V=\frac{1}{2}T_a^3-s_w^2Q_a$, Q_a being the electric charge, and T_a^3 being the weak isospin of the fermions. Here, α is the fine structure constant, s_w and c_w are the sine and cosine of the Weinberg angle, respectively, and $n_c=3$ in QCD. The function λ is defined as $\lambda(z,y,x)=(1-x/z-y/z)^2-4xy/z^2$.

For the gluon fusion subprocess, in the infinite top-mass limit, the Born factor takes the form [37]

$$\hat{\sigma}_{gg}^{(0),\mathrm{EFT}}(Q^2)=\left(\frac{\sqrt{\pi}a_s(\mu_R^2)\alpha}{16s_w^2c_w^2}\right)^2\left(\frac{Q^2}{M_Z^4}\right)\lambda^{\frac{3}{2}}(Q^2,M_H^2,M_Z^2).\tag{2.5}$$

In the infinite top-mass approximation, the full NLO correction to the gluon fusion subprocess is known [37]. In particular, the SV and NSV coefficients up to NLO are given as

$$\begin{aligned}\Delta_\delta^{(1)}&=\left(\frac{56}{27}+8\zeta_2\right)C_A+\frac{64}{9}T_Fn_f+\left(\frac{46}{9}C_A-2\beta_0\right)\ln\left(\frac{\mu_F^2}{Q^2}\right)-2\beta_0\ln\left(\frac{\mu_F^2}{\mu_R^2}\right)+\frac{\hat{\sigma}_{(\mathrm{virt,red})}}{a_s(\mu_R^2)\hat{\sigma}_{gg}^{(0),\mathrm{EFT}}(Q^2)},\\ \Delta_{\mathcal{D}_0}^{(1)}&=-\Delta_{gg,\ln_0}^{(1)}+8C_A=-8C_A\ln\left(\frac{\mu_F^2}{Q^2}\right),\\ \Delta_{\mathcal{D}_1}^{(1)}&=-\Delta_{gg,\ln_1}^{(1)}=16C_A.\end{aligned}\tag{2.6}$$

Here, $\hat{\sigma}_{(\mathrm{virt,red})}$ is the "virtual reducible" contribution arising from Feynman diagrams involving two quark triangles, which in the infinite top-mass limit takes the form [37]

$$\hat{\sigma}_{(\mathrm{virt,red})} = \int d\hat{t} a_s(\mu_R^2) \frac{4}{3}\left(\frac{\sqrt{\pi}a_s(\mu_R^2)\alpha}{16 s_w^2 c_w^2}\right)^2 \frac{1}{\hat{s}M_Z^4}\left\{M_H^2\left(-1+\frac{M_Z^2}{\hat{t}-M_Z^2}+\ln\left(\frac{-\hat{t}}{M_Z^2}\right)\frac{M_Z^2}{\hat{t}-M_Z^2}-\ln\left(\frac{-\hat{t}}{M_Z^2}\right)\frac{M_Z^4}{(\hat{t}-M_Z^2)^2}\right)\right.$$
$$\left.+(\hat{s}-M_Z^2)\left(-1-\frac{M_Z^2}{\hat{t}-M_Z^2}+\ln\left(\frac{-\hat{t}}{M_Z^2}\right)\frac{\hat{t}M_Z^2}{(\hat{t}-M_Z^2)^2}\right)+(\hat{t}\leftrightarrow\hat{u})\right\}, \tag{2.7}$$

where $\hat{u}$ and $\hat{t}$ are the partonic Mandelstam variables.

The Born coefficient in the exact theory, on the other hand, contains Feynman diagrams involving triangle and box diagrams with heavy top-quark dependence. It can be expressed in terms of helicity amplitudes for triangle and box diagrams as

$$\hat{\sigma}_{gg}^{(0)}(Q^2) = \left(\frac{\sqrt{\pi}a_s(\mu_R^2)\alpha}{16 s_w^2}\right)^2 \frac{1}{8\hat{s}^2}\int \mathrm{d}\hat{t} \sum_{\lambda_g,\lambda_g',\lambda_Z} |\mathcal{M}^{\triangle}_{\lambda_g\lambda_g'\lambda_Z} + \mathcal{M}^{\square}_{\lambda_g\lambda_g'\lambda_Z}|^2. \tag{2.8}$$

The exact expression for these helicity amplitudes for two gluons and a Z boson can be found in [33]. These large distributions appearing in Δ^{SV} can be resummed to all orders in the threshold limit $z \to 1$. Typically, resummation is performed in the Mellin N-space, where plus distributions become simple logarithms in the Mellin variable (N). The threshold limit $z \to 1$ translates into the $N \to \infty$ limit. Recently a formalism has been proposed [91–93,109,110] to also resum the NSV logarithms arising out of the diagonal channel. The formalism is built upon a factorization framework that includes a process-dependent hard function, mass factorization kernels, and a soft function, as detailed in [91]. It closely parallels the physical kernel approach of [79], wherein a single logarithmic enhancement in the large-z limit was identified, persisting at all orders in $(1-z)$ near the threshold up to N3LO. This observation motivated the conjecture that such behavior continues to all orders in the strong coupling. Exploiting this conjecture, the authors of [91] established an all-order structure for the soft function. While the structure can be explicitly verified at NLO, the higher-order coefficients are determined using the known fixed-order results for the Higgs [111,112] and DY [113] production processes. In this formalism, the partonic SV and NSV coefficients in the Mellin space can be organized as follows:

$$\frac{1}{\hat{\sigma}_{ab}^{(0)}(Q^2)} Q^2 \frac{\mathrm{d}\hat{\sigma}_{N,ab}^{\overline{\mathrm{N}n\mathrm{LL}}}}{\mathrm{d}Q^2} = \int_0^1 \mathrm{d}z z^{N-1}(\Delta_{ab}^{\mathrm{SV}}(z)+\Delta_{ab}^{\mathrm{NSV}}(z))$$
$$\equiv g_0(Q^2)\exp\left(G_N^{\mathrm{SV}}+G_N^{\mathrm{NSV}}\right). \tag{2.9}$$

The factor g_0 is independent of the Mellin variable and contains process-dependent information. The leading threshold–enhanced large logarithms and the next-to-soft logarithms in Mellin space are resummed through the exponents G_N^{SV} and G_N^{NSV}, respectively. The resummed accuracy is determined through the successive terms from the exponent G_N, which takes the form,

$$G_N^{\mathrm{SV}} = \ln(\bar{N})g_1(\omega) + \sum_{n=1}^{\infty} a_s^{n-1}(\mu_R^2) g_{n+1}(\omega),$$
$$G_N^{\mathrm{NSV}} = \frac{1}{N}\sum_{n=0}^{\infty} a_s^n(\mu_R^2)\left(\bar{g}_{n+1}(\omega) + \sum_{k=0}^{n} h_{nk}(\omega)\ln^k \bar{N}\right), \tag{2.10}$$

where $\bar{N} = N\exp(\gamma_E)$, with γ_E being the Euler-Mascheroni constant and $\omega = 2\beta_0 a_s(\mu_R^2)\ln\bar{N}$. The first term in the expansion of G_N^{SV} corresponds to the leading logarithmic (LL) accuracy, whereas the inclusion of successive terms defines higher accuracies. These coefficients (g_n) are universal and only depend on the partonic flavors being either quark or gluon. In order to obtain $\overline{\mathrm{LL}}$ accuracy in NSV resummation, one has to consider NSV exponents $\bar{g}_1$ and h_{00} in addition to the LL terms. Similarly, for higher accuracies, one has to consider the next terms in the expansion of G_N. Note that starting from NLL ($\overline{\mathrm{NLL}}$), one has to also consider the N-independent g_0 coefficients whose perturbative expansion takes the form

$$g_0(Q^2) = 1 + \sum_{n=1}^{\infty} a_s^n(\mu_R^2) g_{0n}(Q^2). \tag{2.11}$$

The explicit form of the resummed exponent for SV and NSV resummation can be found, e.g., in [51,59]. The SV part of the resummed result obeys the maximally non-Abelian property up to third order, and a generalized form of this property holds beyond that order. In [91], it was further argued that, up to NNLO accuracy, the NSV component of the soft function is universal for both

DY- and Higgs-type processes. We exploit this universality to extract the $\overline{\mathrm{NLL}}$ ingredients from the known results for Higgs production [92]. This implies that the soft (and next-to-soft) gluon contributions at the threshold for the gluon fusion–induced ZH production at NLL ($\overline{\mathrm{NLL}}$) accuracy can be obtained [82] from those of gluon fusion Higgs production, once the respective Born-level and process-dependent virtual contributions are appropriately removed and the Higgs mass is treated as an arbitrary parameter. Up to NLL ($\overline{\mathrm{NLL}}$), one requires the following coefficients:

$$
\begin{aligned}
g_1(\omega) &= \frac{1}{\beta_0}\left\{C_A\left(8\left(1+\frac{\bar{\omega}}{\omega}L_\omega\right)\right)\right\},\\
g_2(\omega) &= \frac{1}{\beta_0^3}\left\{C_A\beta_1(4\omega+4L_\omega+2L_\omega^2)+C_An_f\beta_0\left(\frac{40}{9}(\omega+L_\omega)\right)\right.\\
&\quad\left.+C_A^2\beta_0\left(\left(-\frac{268}{9}+8\zeta_2\right)(\omega+L_\omega)\right)+C_A\beta_0^2\left(4L_\omega\ln\left(\frac{Q^2}{\mu_R^2}\right)+4\omega\ln\left(\frac{\mu_F^2}{\mu_R^2}\right)\right)\right\},\\
\bar{g}_1(\omega) &= \frac{1}{\beta_0}\{C_A(4L_\omega)\},\\
\bar{g}_2(\omega) &= \frac{1}{\bar{\omega}\beta_0^2}\left\{C_AC_Fn_f(-8(\omega+L_\omega))+C_A^2n_f\left(-\frac{40}{3}(\omega+L_\omega)\right)+C_A^3\left(\frac{136}{3}(\omega+L_\omega)\right)\right.\\
&\quad\left.+C_An_f\beta_0\left(\frac{40}{9}\omega\right)+C_A^2\beta_0\left(-\frac{268}{9}+8\zeta_2\right)\omega+C_A\beta_0^2\left(-8+4\ln\left(\frac{Q^2}{\mu_R^2}\right)-4\bar{\omega}\ln\left(\frac{\mu_F^2}{\mu_R^2}\right)\right)\right\},\\
h_{00}(\omega) &= \frac{1}{\beta_0}\{C_A(-8L_\omega)\},\\
h_{10}(\omega) &= \frac{1}{\bar{\omega}\beta_0^2}\left\{C_A\beta_1(-8(\omega+L_\omega))+C_An_f\beta_0\left(-\frac{80}{9}\omega\right)+C_A^2\beta_0\left(\frac{536}{9}-16\zeta_2\right)\omega\right.\\
&\quad\left.+C_A\beta_0^2\left(8-8\ln\left(\frac{Q^2}{\mu_R^2}\right)+8\bar{\omega}\ln\left(\frac{\mu_F^2}{\mu_R^2}\right)\right)\right\},\\
h_{11}(\omega) &= \frac{1}{\bar{\omega}^2\beta_0}\{C_A^2(32\omega\bar{\omega}^2-4\omega)\},
\end{aligned}
\tag{2.12}
$$

where $\bar{\omega}=1-\omega$ and $L_\omega=\ln(\bar{\omega})$. Note that up to the required order $\overline{\mathrm{NLL}}$, the SV and NSV exponents are the same as the ggH case. Up to NLL ($\overline{\mathrm{NLL}}$) accuracy, one also needs the process-dependent coefficient g_{01}, which for the gluon subprocess is found to be

$$
g_{01}(Q^2)=\left(\frac{56}{27}+16\zeta_2\right)C_A+\frac{64}{9}T_Fn_f-2\beta_0\ln\left(\frac{\mu_F^2}{\mu_R^2}\right)+\left(\frac{46}{9}C_A-2\beta_0\right)\ln\left(\frac{\mu_F^2}{Q^2}\right)+\frac{\hat{\sigma}_{(\mathrm{virt,red})}}{a_s(\mu_R^2)\hat{\sigma}_{gg}^{(0)}(Q^2)}. \tag{2.13}
$$

Note that both g_0 and G_N are scheme dependent, which is related to the ambiguity in exponentiation of certain constant terms (e.g., γ_E) coming from Mellin transformation along with the large-N terms (see, e.g., [75] for a detailed discussion). In the context of the LHC, it has been observed that the so-called $\bar{N}$-scheme provides a faster perturbative convergence for the resummed series. In this scheme, the constant g_0 is independent of γ_E.

The resummed result in Eq. (2.9) has to be finally matched with the available fixed-order results to incorporate the hard regular contribution and, at the same time, avoid double counting of SV (NSV) logarithms. The matching with the fixed order is usually performed using the *minimal prescription* [114], and for $\overline{\mathrm{N}n\mathrm{LL}}$ resummation it reads

$$
\begin{aligned}
Q^2\frac{\mathrm{d}\sigma_{ab}^{\mathrm{N}n\mathrm{LO}+\overline{\mathrm{N}n\mathrm{LL}}}}{\mathrm{d}Q^2} &= Q^2\frac{\mathrm{d}\sigma_{ab}^{\mathrm{N}n\mathrm{LO}}}{\mathrm{d}Q^2}+\sum_{ab\in\{gg,q\bar{q}\}}\hat{\sigma}_{ab}^{(0)}(Q^2)\int_{c-i\infty}^{c+i\infty}\frac{\mathrm{d}N}{2\pi i}\tau^{-N}f_{a,N}(\mu_F)f_{b,N}(\mu_F)\\
&\quad\times\left(Q^2\frac{\mathrm{d}\hat{\sigma}_{N,ab}^{\overline{\mathrm{N}n\mathrm{LL}}}}{\mathrm{d}Q^2}-Q^2\frac{\mathrm{d}\hat{\sigma}_{N,ab}^{\overline{\mathrm{N}n\mathrm{LL}}}}{\mathrm{d}Q^2}\bigg|_{\mathrm{tr}}\right).
\end{aligned}
\tag{2.14}
$$

Note that a similar matching procedure is done for the SV resummation. The $f_{a,N}$ are the Mellin-transformed PDFs similar to the partonic coefficient in Eq. (2.9) and can be evolved, e.g., using the publicly available code QCD-PEGASUS [115].

However, for practical purposes, it can also be approximated by directly using the z-space PDF following [47,59]. The subscript "tr" in the last term in the brackets in Eq. (2.14) denotes that the resummed partonic coefficient in Eq. (2.9) has been truncated to the fixed order to avoid double counting the terms already present in the fixed order through $\sigma_{ab}^{\mathrm{N}n\mathrm{LO}}$. Essentially, for SV resummation, this will contain all the fixed-order singular logarithms, and for NSV resummation, it will contain additional NSV terms from the diagonal channel. In the next section, we study the impact of SV and NSV resummation on the gluon subprocess at the LHC.

III. NUMERICAL RESULTS

In this section, we present numerical results for ZH-associated production at the LHC. The default center-of-mass energy of the incoming protons is set to 13.6 TeV. Unless specified otherwise, our numerical analysis employs the `PDF4LHC21_40` [116] PDFs throughout, as provided by `LHAPDF` [117]. In all these cases, the central set is the standard choice. The strong coupling is provided through the `LHAPDF` routine. The fine structure constant is taken as $\alpha \simeq 1/127.93$. The masses of the weak gauge bosons are set to be $M_Z = 91.1880$ GeV and $M_W = 80.3692$ GeV [118] with the corresponding total decay widths of the Z boson, $\Gamma_Z = 2.4955$ GeV. The Weinberg angle is then given by $\sin^2\theta_{\mathrm{w}} = (1 - m_W^2/m_Z^2)$. This corresponds to the weak coupling $G_F \simeq 1.2043993808 \times 10^{-5}$ GeV^{-2}. The mass of the Higgs boson is set to $M_H = 125.2$ GeV.

In the gluon fusion channel, only the top-quark contribution is considered at the lowest order, with the top-quark pole mass set to $m_t = 172.57$ GeV. We also chose the pole mass of the bottom quark to be $m_b = 4.78$ GeV. The unphysical renormalization (μ_R) and factorization scales (μ_F) are set to the invariant mass (Q) of the ZH pair. The scale uncertainties are estimated by simultaneously varying these unphysical scales in the range $[Q/2, 2Q]$ keeping the constraint $|\ln(\mu_R/\mu_F)| < \ln 4$ (known as the seven-point scale uncertainty) and taking the maximum absolute deviation of the cross section from that obtained with the central scale choice. To estimate the impact of the higher-order corrections from fixed order and resummation, we define the following ratios of the cross sections:

$$K_{nm} = \frac{\sigma^{\mathrm{N}n\mathrm{LO}}}{\sigma_c^{\mathrm{N}m\mathrm{LO}}}, \qquad R_{nm} = \frac{\sigma^{\mathrm{N}n\mathrm{LO}+\mathrm{N}n\mathrm{LL}}}{\sigma_c^{\mathrm{N}m\mathrm{LO}}}$$

$$\text{and} \quad \bar{R}_{nm} = \frac{\sigma^{\mathrm{N}n\mathrm{LO}+\overline{\mathrm{N}n\mathrm{LL}}}}{\sigma_c^{\mathrm{N}m\mathrm{LO}}}. \tag{3.1}$$

The subscript "c" in the above expressions indicates that the corresponding quantity is evaluated at the central scale choice. As stated earlier, the lowest-order process for ZH production through the gluon fusion channel contributes at the $\mathcal{O}(\alpha_s^2)$ level, which formally should be considered at N2LO in the perturbation theory. Consequently, we have used the N2LO PDF for the computation of LO and higher-order corrections to the gluon fusion process.

A. Invariant mass distribution

We first look into the invariant mass distribution of the ZH pair. As mentioned in Sec. I, the computation of higher-order corrections is nontrivial due to the involvement of multiple scales, and one can work with EFT to reduce this complexity. For inclusive production of the ZH pair, the total cross section between exact theory and EFT differs by around 31% at LO. However, the difference is more pronounced in the invariant mass distribution, as can be seen from Fig. 1. The band in this plot corresponds to the seven-point scale uncertainty, as described above. Although the differential cross section is comparable in the low invariant mass region, the shape differs significantly in the higher invariant mass region. It is worth noting that in the exact theory at LO, the contribution from the triangular graphs is larger than that of the box diagrams in the low-Q (< 700 GeV) region, however, these two contributions are comparable to each other in the higher-Q region. However, the interference between the triangular and box diagrams is negative and is non-negligible even in the high-Q region. Therefore, it is essential to include the finite quark mass effects to produce the correct behavior for the invariant mass distribution. On the other hand, the total cross section with finite top-quark mass effect at NLO differs only by 5% [45] from the same in EFT. In fact, the exact LO captures the shape of the distribution in bulk, and the effect of top-quark mass on the NLO correction will have less impact on

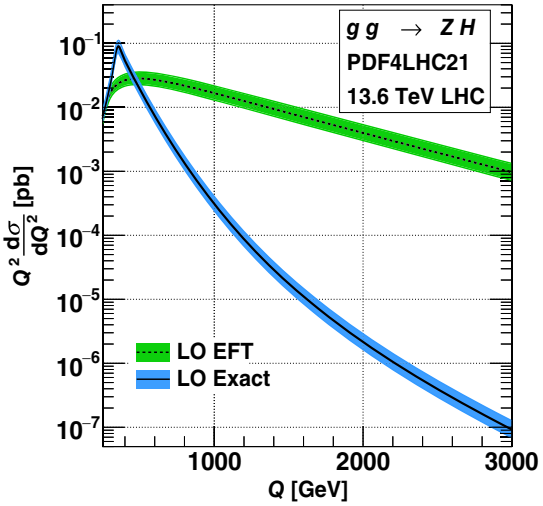


FIG. 1. Invariant mass distribution of ZH for the gluon fusion channel at LO for EFT and exact theories at the 13.6 TeV LHC are presented. The bands correspond to the theoretical uncertainty using seven-point scale variation.

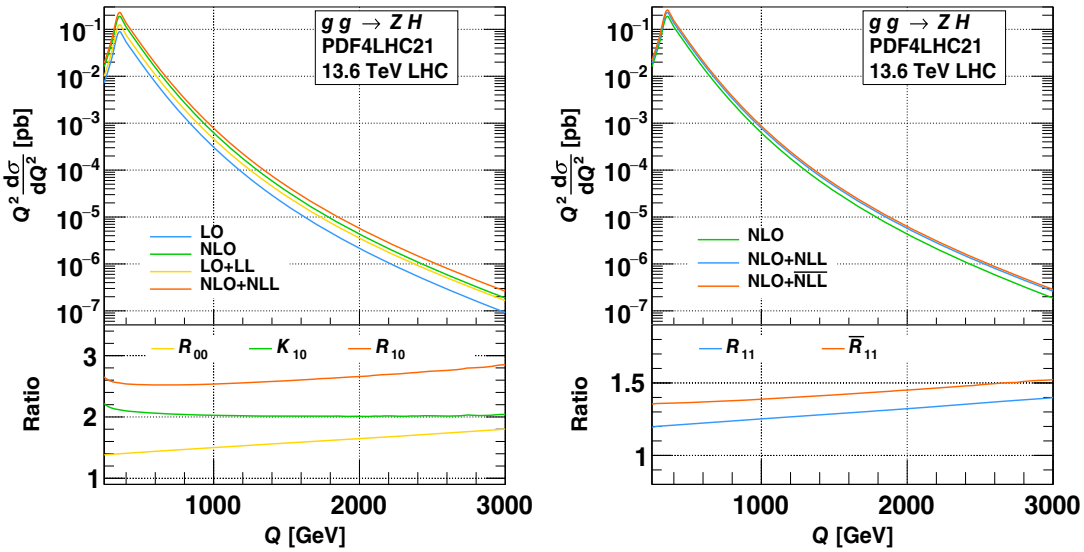


FIG. 2. Comparison between the Born-improved fixed-order and resummed results with corresponding ratios, as defined in Eq. (3.1), are shown here. In the left panel, a comparison between fixed order and SV resummation is shown, and in the right panel, a comparison among fixed order, SV resummation, and NSV resummation is presented.

the shape of the invariant mass distribution.[1] Therefore, working with a Born-improved theory, where the exact LO is rescaled by the NLO K-factor calculated in the EFT, will reduce the complexity while retaining essential features of QCD corrections, in particular the effects of soft radiation, which we are interested in. It is worth noting that although the soft gluon effects themselves are unaffected by the top-quark mass, the latter can still influence the overall distribution. This dependence enters through the process-dependent virtual corrections (encoded in the hard function) as well as through the regular terms beyond the threshold SV/NSV contributions via the fixed-order matching procedure. To evaluate the accuracy of our approximation, we compared the Born-improved NLO cross section with the fully top mass–dependent result of Ref. [44], using identical input settings. We found reasonably good agreement in both the low- and high-Q regions, while deviations of up to about 20% appear in the intermediate-Q range around 1 TeV.[2] In the rest of the article, we use this exact Born-improved EFT NLO cross section for all purposes.

[1]This holds true up to a certain invariant mass region around 1 TeV for the 13.6 TeV LHC. At NLO in the gluon fusion channel, with top-quark dependence, there are also diagrams where a Z boson is radiated from the external light-quark line. Such diagrams contribute at $\mathcal{O}(\alpha_s^3 y_t^2)$ (y_t being the top-quark Yukawa coupling), which is the same order as the gluon fusion subprocess at exact NLO. Their contributions increase from about 1 TeV and could be as large as 10 times [42] the LO results at a higher invariant mass region. However, within the fiducial volume, their impact on the invariant mass distribution is less pronounced.

[2]We thank Stephen Jones for providing benchmark data points for this comparison.

The fixed-order results have been computed with the publicly available code VH@NNLO [23,27,37] and, for resummation, we have developed an in-house code to handle the Mellin inversion described at the end of Sec. II. We first validated our code by reproducing the known results for the total resummed cross section of ZH production up to NLO + NLL accuracy in the N-space formalism [102]. Specifically, we adopted the same parameter choices as in [102], including the renormalization and factorization scales, parton distribution functions, prescription for the inverse Mellin transform, and the Landau-pole regularization scheme. We found excellent agreement with the published results, within the expected numerical integration uncertainties. We further reproduced the known result for the inclusive resummed Higgs cross section up to NLO + NLL both in N- and $\bar{N}$-schemes. As discussed in Sec. II, the $\bar{N}$-scheme offers a faster perturbative convergence with a better control on the scale uncertainty, and we chose to use this scheme for all of our studies in this article.

In the left panel of Fig. 2, we compare the SV resummation with the fixed-order result up to NLO (NLL) level, and we observe the expected behavior of better perturbative convergence for the SV resummed series. This is further evidenced from the lower inset where the ratios are displayed. From the ratio K_{10}, it is evident that the NLO correction can reach to around 100% compared to LO across most of the kinematic region considered. The LO + LL correction captures a significant portion of the higher-order effects and provides an additional contribution of 80% of the LO, particularly in the high invariant mass region ($Q = 3000$ GeV). This clearly demonstrates that the soft gluon effect is dominant for this

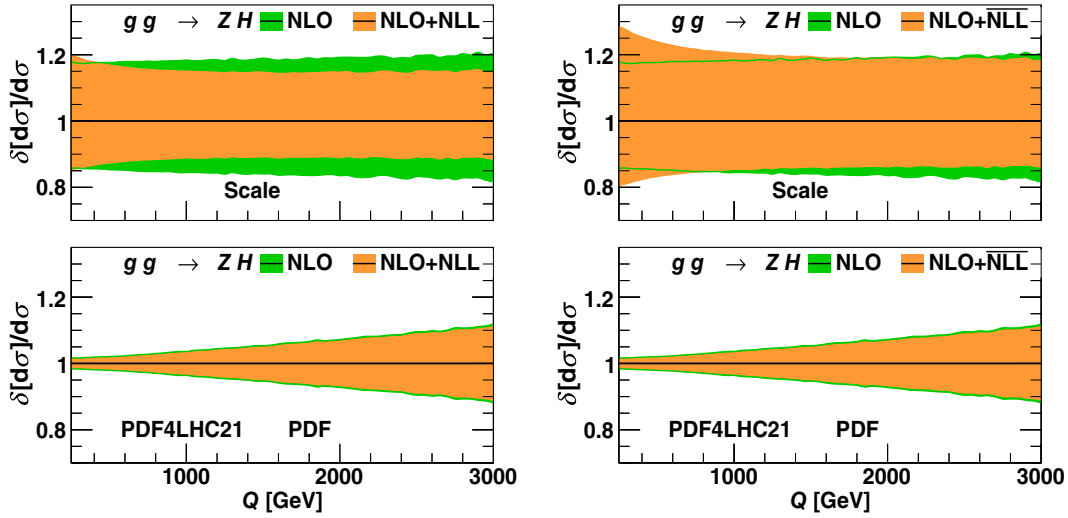


FIG. 3. The seven-point scale uncertainty (upper panel) and the PDF uncertainty (lower panel) of gluon fusion ZH production are compared for Born-improved SV (left) and NSV resummation (right) against their corresponding fixed-order results at the 13.6 TeV LHC.

process. The NLO + NLL correction also shows a significant enhancement (through the R_{10} factor), reaching around 2.8 times the LO, particularly in the high invariant mass region. In the right panel of Fig. 2, we further compare the NLO (NLL) results with the new $\overline{\text{NLL}}$ results. Through the ratios R_{11} and $\bar{R}_{11}$ in the bottom panel there, we observe that NLO + NLL corrections account for about 20% of NLO in the low invariant mass region and rise to approximately 40% in the high invariant mass region. The NSV resummation at NLO + $\overline{\text{NLL}}$, on the other hand, contributes an additional 12%–15% correction over NLO + NLL across most of the invariant mass region.

In Fig. 3, we have also analyzed different sources of uncertainties in these predictions. In general, the scale uncertainties at NLO are around 20%, which gets reduced to around 15% in NLO + NLL distribution, particularly in the high invariant mass region, as shown in the left panel of Fig. 3. In contrast, the NSV resummation at NLO + $\overline{\text{NLL}}$ does not show similar scale reduction over NLO, particularly in the low invariant mass region. In the high invariant mass region, it marginally improves the scale uncertainty over the NLO results. In the bottom panels of Fig. 3, we compare the PDF uncertainties for both SV and NSV resummed cases against the fixed order. These uncertainties generally increase with Q, as PDFs are well constrained in the intermediate-x region relevant to the ZH threshold production, whereas at large-x, these are poorly constrained, resulting in significant uncertainties of around 10% at NLO in the high-Q region. The SV and NSV resummed results show marginal improvements in PDF uncertainties by around 0.8% over the NLO.

$$Q^2\frac{\mathrm{d}\sigma_{pp}^{\mathrm{N3LO}}}{\mathrm{d}Q^2}=Q^2\frac{\mathrm{d}\sigma_{\mathrm{DY}}^{\mathrm{N3LO}}}{\mathrm{d}Q^2}+Q^2\frac{\mathrm{d}\sigma_{gg}^{\mathrm{NLO}}}{\mathrm{d}Q^2},$$
$$Q^2\frac{\mathrm{d}\sigma_{pp}^{\mathrm{N3LO+N3LL}}}{\mathrm{d}Q^2}=Q^2\frac{\mathrm{d}\sigma_{\mathrm{DY}}^{\mathrm{N3LO+N3LL}}}{\mathrm{d}Q^2}+Q^2\frac{\mathrm{d}\sigma_{gg}^{\mathrm{NLO+NLL}}}{\mathrm{d}Q^2}. \quad (3.2)$$

For completeness, we now combine the gluon fusion results with other subprocesses for ZH contribution to obtain full $pp \to ZH$ results at the $\mathcal{O}(\alpha_s^3)$ level. Particularly, in the fixed-order case, we combine the contributions arising from the DY-type channel with that from the gluon fusion channel at $\mathcal{O}(\alpha_s^3)$, as given in Eq. (3.2). For the resummation case, we chose to use the SV resummed results. While NSV resummation shows some enhancement over the SV resummed results (as seen from Fig. 2), it still lacks contributions from off-diagonal channels. Moreover, one would also require the NSV accuracy for the DY-type subprocess for which the relevant ingredients are still missing. Hence, we combine the fixed-order results with SV resummed results for both DY-type and gluon fusion channels. The required N3LO+N3LL SV resummed results for the DY-type channel were obtained [100] by us a few years ago. In the left panel of Fig. 4, we show these results separately for both DY-type and gluon fusion channels along with the scale uncertainties. Note that the relative scale uncertainty for the DY type is not visible on the scale of this plot. The right panel of Fig. 4 shows the combined results for invariant mass distribution at N3LO and N3LO +N3LL. The bottom panel highlights the enhancement from N3LO through the K_{33} and R_{33} factors. In Fig. 5, we show the scale and PDF uncertainties for the combined results at N3LO+N3LL. The PDF uncertainty increases with Q, reaching around 10% in the high invariant mass

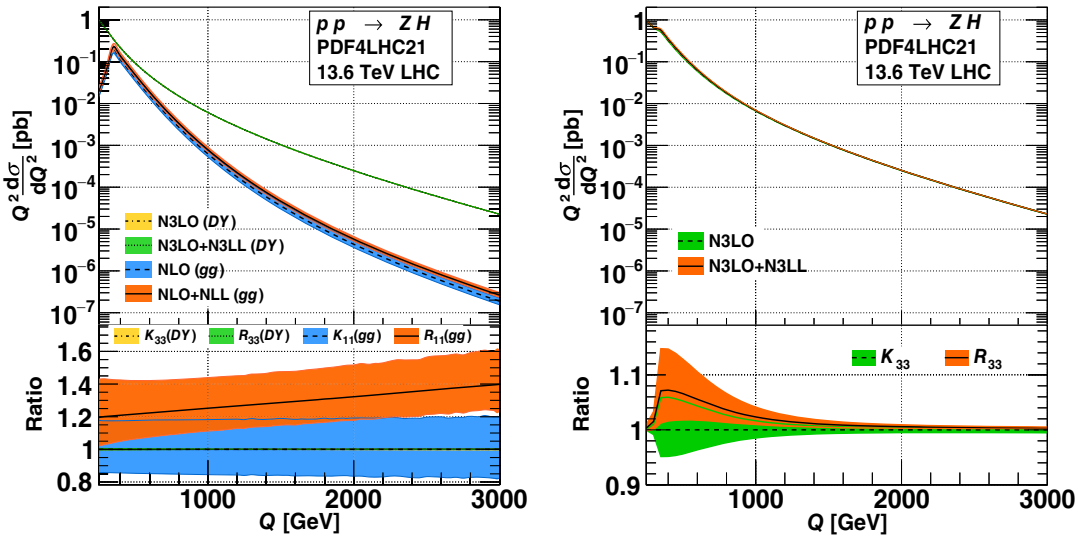


FIG. 4. Left: the contributions from DY and gluon subprocesses are shown for fixed-order and SV resummed cases with the corresponding ratios at the bottom and the uncertainty from the scale variation. Right: the combined contribution at the highest accuracy for the fixed order and the SV resummed order are shown along with the scale uncertainties.

region. On the other hand, the scale uncertainty is largest at the top threshold ($Q \sim 2m_t$), reaching up to 6% and decreasing significantly in the high-Q region, reducing to as low as 0.1%.

B. Total cross section

Finally, we also present the total cross section for the resummed results by integrating the invariant mass distributions up to $\sqrt{S}$. Table I provides the total cross sections for the gluon fusion channel at fixed order and at SV and NSV resummation. Alongside, we provide a detailed assessment of the theoretical uncertainties arising from the standard seven-point scale variation, the choice of nonperturbative PDF sets, and the variation of the strong coupling constant $\alpha_s(M_Z)$. For the latter, we follow the PDF4LHC recommendations and employ the `PDF4LHC21_40_pdfas` set, utilizing subsets 41 and 42, which correspond to $\alpha_s^-(M_Z) = 0.117$ and $\alpha_s^+(M_Z) = 0.119$, respectively. The central value is taken as $\alpha_s^c(M_Z) = 0.118$, consistent with the PDF set. A 1σ variation of ± 0.0015 is applied to estimate the associated uncertainty, computed as $\delta(\alpha_s) = \pm 3/4|\sigma(\alpha_s^+(M_Z)) - \sigma(\alpha_s^-(M_Z))|/\sigma(\alpha_s^c(M_Z))$. Additionally, we also present the combined uncertainties from PDF and α_s by adding the respective errors in quadrature. The largest source of uncertainty arises from the scale variation, which at the NLO + NLL level is around 19.4%, indicating the need for further improvements through higher-order computation.

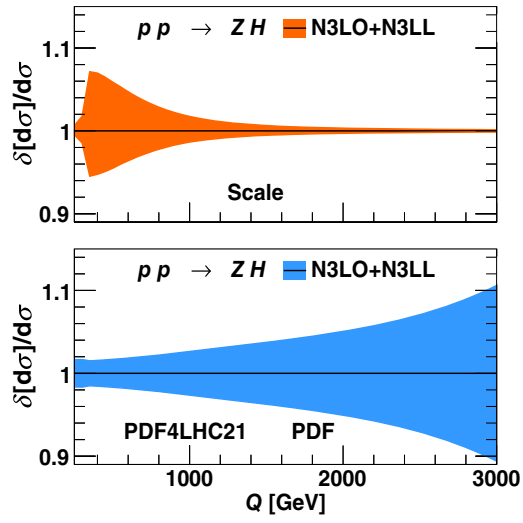


FIG. 5. The seven-point scale uncertainty (upper panel) and the PDF uncertainty (lower panel) are shown for the $pp \to ZH$ process at the 13.6 TeV LHC.

In Table II, we present the total production cross sections of ZH at the LHC by combining contributions from different channels. Particularly, in the fixed-order case, we combine the contributions arising from the DY-type channel ($\sigma_{\rm DY}^{\rm N3LO}$), the bottom quark–initiated t-channel ($\sigma_{b\bar{b}}$), the gluon fusion channel ($\sigma_{gg}^{\rm NLO}$), and contribution coming from Higgs radiation from the top-quark loop in the quark annihilation channel [$\sigma_{\rm top}(a_s^2)$], as described in Sec. I and defined as

$$\begin{aligned}\sigma_{\rm tot}^{\rm N3LO} &= \sigma_{\rm DY}^{\rm N3LO} + \sigma_{gg}^{\rm NLO} + \sigma_{\rm top}(a_s^2) + \sigma_{b\bar{b}},\\ \sigma_{\rm tot}^{\rm N3LO+N3LL} &= \sigma_{\rm DY}^{\rm N3LO+N3LL} + \sigma_{gg}^{\rm NLO+NLL} + \sigma_{\rm top}(a_s^2) + \sigma_{b\bar{b}}.\end{aligned} \tag{3.3}$$

For the resummation case, we improve the fixed order for the DY-type channel by SV resummation at N3LO+ N3LL

TABLE I. The ZH production cross sections (in fb) are presented at exact LO, and Born-improved NLO, along with corresponding SV and NSV resummed results at the 13.6 TeV LHC with the seven-point scale, PDF, and α_s uncertainties.

Order	Cross section (fb)	Scale	δ (PDF)	$\delta(\alpha_s)$	δ (PDF $+ \alpha_s$)
$\sigma_{gg}^{\mathrm{LO}}$	60.25	$\pm 24.6\%$	$\pm 0.68\%$	$\pm 1.47\%$	$\pm 1.62\%$
$\sigma_{gg}^{\mathrm{NLO}}$	124.74	$\pm 15.3\%$	$\pm 0.71\%$	$\pm 1.97\%$	$\pm 2.09\%$
$\sigma_{gg}^{\mathrm{LO+LL}}$	84.74	$\pm 27.5\%$	$\pm 0.69\%$	$\pm 1.79\%$	$\pm 1.92\%$
$\sigma_{gg}^{\mathrm{NLO+NLL}}$	151.30	$\pm 19.4\%$	$\pm 0.71\%$	$\pm 2.28\%$	$\pm 2.39\%$
$\sigma_{gg}^{\mathrm{LO+\overline{LL}}}$	96.27	$\pm 29.3\%$	$\pm 0.69\%$	$\pm 1.95\%$	$\pm 2.07\%$
$\sigma_{gg}^{\mathrm{NLO+\overline{NLL}}}$	170.73	$\pm 27.0\%$	$\pm 0.71\%$	$\pm 2.51\%$	$\pm 2.61\%$

TABLE II. The ZH production cross-section (in pb) are presented for DY-type and total [defined in Eq. (3.3)] at order N3LO and N3LO+N3LL for 13.6 TeV LHC with seven-point scale, PDF and α_s uncertainties.

Order	Cross section (pb)	Scale	δ (PDF)	$\delta(\alpha_s)$	δ (PDF $+ \alpha_s$)
$\sigma_{\mathrm{DY}}^{\mathrm{N3LO}}$	0.8416	$\pm 0.28\%$	$\pm 0.77\%$	$\pm 0.79\%$	$\pm 1.10\%$
$\sigma_{\mathrm{DY}}^{\mathrm{N3LO+N3LL}}$	0.8416	$\pm 0.55\%$	$\pm 0.77\%$	$\pm 0.78\%$	$\pm 1.10\%$
$\sigma_{\mathrm{tot}}^{\mathrm{N3LO}}$	0.9776	$\pm 1.94\%$	$\pm 0.65\%$	$\pm 0.96\%$	$\pm 1.16\%$
$\sigma_{\mathrm{tot}}^{\mathrm{N3LO+N3LL}}$	1.0042	$\pm 2.98\%$	$\pm 0.63\%$	$\pm 1.03\%$	$\pm 1.21\%$

and for the gluon channel by resummation at NLO + NLL. For the DY-type channel, resummation has very little effect in this order and the major improvement is obtained through the gluon fusion channel. For the total cross section, the resummation improves the cross section by around 2.7% compared to the fixed order, whereas the scale uncertainty increases by 1%. This can be traced to the fact that the total cross section receives significant contributions from the low invariant mass region, where the factorization scale uncertainty remains significant. However, all other sources of uncertainties remain small, contributing less than 1%.

IV. CONCLUSION

To summarize, we have investigated the impact of soft gluon resummation on the ZH production process in the gluon fusion channel at the LHC. In the low invariant mass region, near the top-pair threshold ($Q \sim 2m_t$), the gluon fusion channel at the $\mathcal{O}(\alpha_s^2)$ level contributes around 20% of the dominant DY-type channel, highlighting its significance and the necessity of including its contribution.

We first obtained the Born-improved NLO corrections by rescaling the exact LO results with the mass-dependent NLO K-factor obtained from the effective theory. Using the universal cusp anomalous dimensions, splitting kernels, we performed the SV and the NSV resummation and presented numerical results for the invariant mass distribution as well as the production cross sections to NLO + NLL ($\overline{\mathrm{NLL}}$) accuracy for the current LHC energies. The NLO corrections contribute as large as 100% of LO for the total ZH production cross section in the gluon fusion channel. We observed that the SV (NSV) resummation contributes an additional 19.4% (35.3%) at the NLL ($\overline{\mathrm{NLL}}$) level over NLO in the low-Q region. In the high invariant mass region (around $Q = 3000$ GeV), the SV (NSV) resummation reduces the seven-point scale uncertainties at NLO level by a few percent, 5.0%(1.4%). Besides the scale uncertainties, we also quantified the uncertainties due to the PDFs on resummed results, and these were found to be around 1.6% in the low invariant mass region.

Finally, for experimental analysis, we combined the contributions from different subprocesses, including the soft gluon resummation effects, and presented comprehensive results for the invariant mass distribution as well as the total production cross sections at the LHC. We note that except for the uncertainties due to the nonperturbative inputs from PDFs, the theoretical uncertainties in the high invariant mass region are well under control. However, to advance the precision for this process further, the higher-order corrections beyond NLO for the gluon fusion channel will be essential.

ACKNOWLEDGMENTS

We thank Pulak Banerjee for the useful discussion. G. D. also thanks Aparna Sankar for helpful communication. The research of G. D. is supported by the Deutsche Forschungsgemeinschaft (DFG, German Research Foundation) under grant 396021762-TRR 257 (Particle Physics Phenomenology after Higgs discovery). The research work of M. C. K. is supported by the SERB Core Research Grant (CRG) under the project CRG/2021/005270. The research work of K. S. is supported by the Royal Society (URF/R/231031) and the STFC (ST/X003167/1 and ST/X000745/1). The computation has been performed on the OMNI cluster at the University of Siegen, and on the ParamIshan cluster computing facility at IIT Guwahati.

DATA AVAILABILITY

The data are not publicly available. The data are available from the authors upon reasonable request.

[1] F. Englert and R. Brout, Broken symmetry and the mass of gauge vector mesons, Phys. Rev. Lett. **13**, 321 (1964).
[2] P. W. Higgs, Broken symmetries and the masses of gauge bosons, Phys. Rev. Lett. **13**, 508 (1964).
[3] G. S. Guralnik, C. R. Hagen, and T. W. B. Kibble, Global conservation laws and massless particles, Phys. Rev. Lett. **13**, 585 (1964).
[4] G. Aad *et al.* (ATLAS Collaboration), Observation of a new particle in the search for the standard model Higgs boson with the ATLAS detector at the LHC, Phys. Lett. B **716**, 1 (2012).
[5] S. Chatrchyan *et al.* (CMS Collaboration), Observation of a new boson at a mass of 125 GeV with the CMS experiment at the LHC, Phys. Lett. B **716**, 30 (2012).
[6] C. Englert, M. McCullough, and M. Spannowsky, Gluon-initiated associated production boosts Higgs physics, Phys. Rev. D **89**, 013013 (2014).
[7] B. Hespel, F. Maltoni, and E. Vryonidou, Higgs and Z boson associated production via gluon fusion in the SM and the 2HDM, J. High Energy Phys. 06 (2015) 065.
[8] D. Goncalves, F. Krauss, S. Kuttimalai, and P. Maierhöfer, Higgs-strahlung: Merging the NLO Drell-Yan and loop-induced $0+1$ jet multiplicities, Phys. Rev. D **92**, 073006 (2015).
[9] M. Aaboud *et al.* (ATLAS Collaboration), Measurement of VH, $H \to b\bar{b}$ production as a function of the vector-boson transverse momentum in 13 TeV pp collisions with the ATLAS detector, J. High Energy Phys. 05 (2019) 141.
[10] G. Aad *et al.* (ATLAS Collaboration), Measurement of the associated production of a Higgs boson decaying into b-quarks with a vector boson at high transverse momentum in pp collisions at $\sqrt{s} = 13$ TeV with the ATLAS detector, Phys. Lett. B **816**, 136204 (2021).
[11] G. Aad *et al.* (ATLAS Collaboration), Measurements of WH and ZH production in the $H \to b\bar{b}$ decay channel in pp collisions at 13 TeV with the ATLAS detector, Eur. Phys. J. C **81**, 178 (2021).
[12] CMS Collaboration, Combined Higgs boson production and decay measurements with up to 137 fb^{-1} of proton-proton collision data at $\sqrt{s} = 13$ TeV, Report No. CMS-PAS-HIG-19-005, 2020, https://cds.cern.ch/record/2706103.
[13] ATLAS Collaboration, Combination of measurements of Higgs boson production in association with a W or Z boson in the $b\bar{b}$ decay channel with the ATLAS experiment at $\sqrt{s} = 13$ TeV, Report No. ATLAS-CONF-2021-051, 2021, https://cds.cern.ch/record/2782535.
[14] V. Chekhovsky *et al.* (CMS Collaboration), Constraints on standard model effective field theory for a Higgs boson produced in association with W or Z bosons in the $H \to b\bar{b}$ decay channel in proton-proton collisions at $\sqrt{s} = 13$ TeV, arXiv:2411.16907.
[15] A. Hayrapetyan *et al.* (CMS Collaboration), Study of WH production through vector boson scattering and extraction of the relative sign of the W and Z couplings to the Higgs boson in proton-proton collisions at $\sqrt{s} = 13$ TeV, arXiv:2405.16566.
[16] A. Hayrapetyan *et al.* (CMS Collaboration), Search for ZZ and ZH production in the $b\bar{b}b\bar{b}$ final state using proton-proton collisions at $\sqrt{s} = 13$ TeV, Eur. Phys. J. C **84**, 712 (2024).
[17] A. Hayrapetyan *et al.* (CMS Collaboration), Search for Higgs boson pair production with one associated vector boson in proton-proton collisions at $\sqrt{s} = 13$ TeV, J. High Energy Phys. 10 (2024) 061.
[18] A. Tumasyan *et al.* (CMS Collaboration), Measurement of simplified template cross sections of the Higgs boson produced in association with W or Z bosons in the $H \to bb^{-}$ decay channel in proton-proton collisions at s=13 TeV, Phys. Rev. D **109**, 092011 (2024).
[19] G. Aad *et al.* (ATLAS Collaboration), Measurements of WH and ZH production with Higgs boson decays into bottom quarks and direct constraints on the charm Yukawa coupling in 13 TeV pp collisions with the ATLAS detector, arXiv:2410.19611.
[20] T. Han and S. Willenbrock, QCD correction to the $pp \to WH$ and ZH total cross-sections, Phys. Lett. B **273**, 167 (1991).
[21] O. Brein, A. Djouadi, and R. Harlander, NNLO QCD corrections to the Higgs-strahlung processes at hadron colliders, Phys. Lett. B **579**, 149 (2004).
[22] O. Brein, M. Ciccolini, S. Dittmaier, A. Djouadi, R. Harlander, and M. Kramer, Precision calculations for

associated WH and ZH production at hadron colliders, in *3rd Les Houches Workshop on Physics at TeV Colliders* (2004), arXiv:hep-ph/0402003.
[23] O. Brein, R. V. Harlander, and T. J. E. Zirke, VH@NNLO—Higgs Strahlung at hadron colliders, Comput. Phys. Commun. **184**, 998 (2013).
[24] G. Ferrera, M. Grazzini, and F. Tramontano, Associated ZH production at hadron colliders: The fully differential NNLO QCD calculation, Phys. Lett. B **740**, 51 (2015).
[25] J. M. Campbell, R. K. Ellis, and C. Williams, Associated production of a Higgs boson at NNLO, J. High Energy Phys. 06 (2016) 179.
[26] G. Ferrera, G. Somogyi, and F. Tramontano, Associated production of a Higgs boson decaying into bottom quarks at the LHC in full NNLO QCD, Phys. Lett. B **780**, 346 (2018).
[27] R. V. Harlander, J. Klappert, S. Liebler, and L. Simon, VH@NNLO-v2: New physics in Higgs Strahlung, J. High Energy Phys. 05 (2018) 089.
[28] J. Baglio, C. Duhr, B. Mistlberger, and R. Szafron, Inclusive production cross sections at N3LO, arXiv:2209.06138.
[29] T. Ahmed, A. H. Ajjath, L. Chen, P. K. Dhani, P. Mukherjee, and V. Ravindran, Polarised amplitudes and soft-virtual cross sections for $b\bar{b} \to ZH$ at NNLO in QCD, J. High Energy Phys. 01 (2020) 030.
[30] M. L. Ciccolini, S. Dittmaier, and M. Kramer, Electroweak radiative corrections to associated WH and ZH production at hadron colliders, Phys. Rev. D **68**, 073003 (2003).
[31] A. Denner, S. Dittmaier, S. Kallweit, and A. Muck, Electroweak corrections to Higgs-strahlung off W/Z bosons at the Tevatron and the LHC with HAWK, J. High Energy Phys. 03 (2012) 075.
[32] O. Brein, R. Harlander, M. Wiesemann, and T. Zirke, Top-quark mediated effects in hadronic Higgs-Strahlung, Eur. Phys. J. C **72**, 1868 (2012).
[33] B. A. Kniehl and C. P. Palisoc, Associated production of Z and neutral Higgs bosons at the CERN Large Hadron Collider, Phys. Rev. D **85**, 075027 (2012).
[34] D. A. Dicus and C. Kao, Higgs boson—Z^0 production from gluon fusion, Phys. Rev. D **38**, 1008 (1988).
[35] B. A. Kniehl, Associated production of Higgs and Z bosons from gluon fusion in hadron collisions, Phys. Rev. D **42**, 2253 (1990).
[36] B. A. Kniehl, On the decay mode Z → H gg, Phys. Rev. D **42**, 3100 (1990).
[37] L. Altenkamp, S. Dittmaier, R. V. Harlander, H. Rzehak, and T. J. E. Zirke, Gluon-induced Higgs-strahlung at next-to-leading order QCD, J. High Energy Phys. 02 (2013) 078.
[38] A. Hasselhuhn, T. Luthe, and M. Steinhauser, On top quark mass effects to $gg \to ZH$ at NLO, J. High Energy Phys. 01 (2017) 073.
[39] J. Davies, G. Mishima, and M. Steinhauser, Virtual corrections to $gg \to ZH$ in the high-energy and large-m_t limits, J. High Energy Phys. 03 (2021) 034.
[40] L. Alasfar, G. Degrassi, P. P. Giardino, R. Gröber, and M. Vitti, Virtual corrections to $gg \to ZH$ via a transverse momentum expansion, J. High Energy Phys. 05 (2021) 168.
[41] L. Bellafronte, G. Degrassi, P. P. Giardino, R. Groeber, and M. Vitti, Gluon fusion production at NLO: Merging the transverse momentum and the high-energy expansions, J. High Energy Phys. 07 (2022) 069.
[42] G. Degrassi, R. Gröber, M. Vitti, and X. Zhao, On the NLO QCD corrections to gluon-initiated ZH production, J. High Energy Phys. 08 (2022) 009.
[43] G. Wang, X. Xu, Y. Xu, and L. L. Yang, Next-to-leading order corrections for $gg \to ZH$ with top quark mass dependence, Phys. Lett. B **829**, 137087 (2022).
[44] L. Chen, G. Heinrich, S. P. Jones, M. Kerner, J. Klappert, and J. Schlenk, ZH production in gluon fusion: two-loop amplitudes with full top quark mass dependence, J. High Energy Phys. 03 (2021) 125.
[45] L. Chen, J. Davies, G. Heinrich, S. P. Jones, M. Kerner, G. Mishima, J. Schlenk, and M. Steinhauser, ZH production in gluon fusion at NLO in QCD, J. High Energy Phys. 08 (2022) 056.
[46] G. F. Sterman, Summation of large corrections to short distance hadronic cross-sections, Nucl. Phys. **B281**, 310 (1987).
[47] S. Catani and L. Trentadue, Resummation of the QCD perturbative series for hard processes, Nucl. Phys. **B327**, 323 (1989).
[48] S. Catani and L. Trentadue, Comment on QCD exponentiation at large x, Nucl. Phys. **B353**, 183 (1991).
[49] N. Kidonakis and G. F. Sterman, Resummation for QCD hard scattering, Nucl. Phys. **B505**, 321 (1997).
[50] N. Kidonakis, A unified approach to NNLO soft and virtual corrections in electroweak, Higgs, QCD, and SUSY processes, Int. J. Mod. Phys. A **19**, 1793 (2004).
[51] S. Moch, J. A. M. Vermaseren, and A. Vogt, Higher-order corrections in threshold resummation, Nucl. Phys. B **726**, 317 (2005).
[52] E. Laenen and L. Magnea, Threshold resummation for electroweak annihilation from DIS data, Phys. Lett. B **632**, 270 (2006).
[53] N. Kidonakis, Next-to-next-to-next-to-leading-order soft-gluon corrections in hard-scattering processes near threshold, Phys. Rev. D **73**, 034001 (2006).
[54] V. Ravindran, On Sudakov and soft resummations in QCD, Nucl. Phys. **B746**, 58 (2006).
[55] V. Ravindran, Higher-order threshold effects to inclusive processes in QCD, Nucl. Phys. **B752**, 173 (2006).
[56] A. Idilbi, X.-d. Ji, and F. Yuan, Resummation of threshold logarithms in effective field theory for DIS, Drell-Yan and Higgs production, Nucl. Phys. **B753**, 42 (2006).
[57] T. Becher, M. Neubert, and B. D. Pecjak, Factorization and momentum-space resummation in deep-inelastic scattering, J. High Energy Phys. 01 (2007) 076.
[58] T. Ahmed, A. H. Ajjath, G. Das, P. Mukherjee, V. Ravindran, and S. Tiwari, Soft-virtual correction and threshold resummation for n-colorless particles to fourth order in QCD: Part I, arXiv:2010.02979.
[59] S. Catani, D. de Florian, M. Grazzini, and P. Nason, Soft gluon resummation for Higgs boson production at hadron colliders, J. High Energy Phys. 07 (2003) 028.

[60] S. Moch and A. Vogt, Higher-order soft corrections to lepton pair and Higgs boson production, Phys. Lett. B **631**, 48 (2005).
[61] D. de Florian and J. Zurita, Soft-gluon resummation for pseudoscalar Higgs boson production at hadron colliders, Phys. Lett. B **659**, 813 (2008).
[62] N. Kidonakis, Collinear and soft gluon corrections to Higgs production at NNNLO, Phys. Rev. D **77**, 053008 (2008).
[63] S. Catani, L. Cieri, D. de Florian, G. Ferrera, and M. Grazzini, Threshold resummation at N^3LL accuracy and soft-virtual cross sections at N^3LO, Nucl. Phys. **B888**, 75 (2014).
[64] M. Bonvini and S. Marzani, Resummed Higgs cross section at N^3LL, J. High Energy Phys. 09 (2014) 007.
[65] T. Ahmed, G. Das, M. C. Kumar, N. Rana, and V. Ravindran, RG improved Higgs boson production to N^3LO in QCD, arXiv:1505.07422.
[66] T. Schmidt and M. Spira, Higgs boson production via gluon fusion: Soft-gluon resummation including mass effects, Phys. Rev. D **93**, 014022 (2016).
[67] T. Ahmed, M. Bonvini, M. C. Kumar, P. Mathews, N. Rana, V. Ravindran, and L. Rottoli, Pseudo-scalar Higgs boson production at $N^3LO_A + N^3LL'$, Eur. Phys. J. C **76**, 663 (2016).
[68] M. Bonvini, S. Marzani, C. Muselli, and L. Rottoli, On the Higgs cross section at $N^3LO + N^3LL$ and its uncertainty, J. High Energy Phys. 08 (2016) 105.
[69] N. Kidonakis, Higher-order radiative corrections for $b\bar{b} \to H^- W^+$, Phys. Rev. D **97**, 034002 (2018).
[70] A. A H, A. Chakraborty, G. Das, P. Mukherjee, and V. Ravindran, Resummed prediction for Higgs boson production through $b\bar{b}$ annihilation at N^3LL, J. High Energy Phys. 11 (2019) 006.
[71] G. Das, S.-O. Moch, and A. Vogt, Soft corrections to inclusive deep-inelastic scattering at four loops and beyond, J. High Energy Phys. 03 (2020) 116.
[72] G. Das, M. C. Kumar, and K. Samanta, Resummed inclusive cross-section in ADD model at N^3LL, J. High Energy Phys. 10 (2020) 161.
[73] G. Das, M. C. Kumar, and K. Samanta, Resummed inclusive cross-section in Randall-Sundrum model at NNLO + NNLL, J. High Energy Phys. 07 (2020) 040.
[74] G. Das, M. C. Kumar, and K. Samanta, Precision QCD phenomenology of exotic spin-2 search at the LHC, J. High Energy Phys. 04 (2021) 111.
[75] A. A H, G. Das, M. C. Kumar, P. Mukherjee, V. Ravindran, and K. Samanta, Resummed Drell-Yan cross-section at N^3LL, J. High Energy Phys. 10 (2020) 153.
[76] A. A H and H.-S. Shao, $N^3LO + N^3LL$ QCD improved Higgs pair cross sections, J. High Energy Phys. 02 (2023) 067.
[77] P. Banerjee, C. Dey, M. C. Kumar, and V. Pandey, Threshold resummation for Z-boson pair production at NNLO + NNLL, arXiv:2409.16375.
[78] N. Kidonakis and G. F. Sterman, Subleading logarithms in QCD hard scattering, Phys. Lett. B **387**, 867 (1996).
[79] S. Moch and A. Vogt, On non-singlet physical evolution kernels and large-x coefficient functions in perturbative QCD, J. High Energy Phys. 11 (2009) 099.
[80] G. Soar, S. Moch, J. A. M. Vermaseren, and A. Vogt, On Higgs-exchange DIS, physical evolution kernels and fourth-order splitting functions at large x, Nucl. Phys. **B832**, 152 (2010).
[81] D. Bonocore, E. Laenen, L. Magnea, S. Melville, L. Vernazza, and C. D. White, A factorization approach to next-to-leading-power threshold logarithms, J. High Energy Phys. 06 (2015) 008.
[82] V. Del Duca, E. Laenen, L. Magnea, L. Vernazza, and C. D. White, Universality of next-to-leading power threshold effects for colourless final states in hadronic collisions, J. High Energy Phys. 11 (2017) 057.
[83] M. Beneke, A. Broggio, M. Garny, S. Jaskiewicz, R. Szafron, L. Vernazza, and J. Wang, Leading-logarithmic threshold resummation of the Drell-Yan process at next-to-leading power, J. High Energy Phys. 03 (2019) 043.
[84] N. Bahjat-Abbas, D. Bonocore, J. Sinninghe Damsté, E. Laenen, L. Magnea, L. Vernazza, and C. D. White, Diagrammatic resummation of leading-logarithmic threshold effects at next-to-leading power, J. High Energy Phys. 11 (2019) 002.
[85] M. Beneke, A. Broggio, S. Jaskiewicz, and L. Vernazza, Threshold factorization of the Drell-Yan process at next-to-leading power, J. High Energy Phys. 07 (2020) 078.
[86] M. Beneke, M. Garny, S. Jaskiewicz, R. Szafron, L. Vernazza, and J. Wang, Leading-logarithmic threshold resummation of Higgs production in gluon fusion at next-to-leading power, J. High Energy Phys. 01 (2020) 094.
[87] I. Moult, I. W. Stewart, and G. Vita, Subleading power factorization with radiative functions, J. High Energy Phys. 11 (2019) 153.
[88] Z. L. Liu, B. Mecaj, M. Neubert, and X. Wang, Factorization at subleading power, Sudakov resummation, and endpoint divergences in soft-collinear effective theory, Phys. Rev. D **104**, 014004 (2021).
[89] M. van Beekveld, W. Beenakker, R. Basu, E. Laenen, A. Misra, and P. Motylinski, Next-to-leading power threshold effects for resummed prompt photon production, Phys. Rev. D **100**, 056009 (2019).
[90] G. Das, S. Moch, and A. Vogt, Approximate four-loop QCD corrections to the Higgs-boson production cross section, Phys. Lett. B **807**, 135546 (2020).
[91] A. A H, P. Mukherjee, and V. Ravindran, Next to soft corrections to Drell-Yan and Higgs boson productions, Phys. Rev. D **105**, 094035 (2022).
[92] A. A H, P. Mukherjee, V. Ravindran, A. Sankar, and S. Tiwari, Resummed Higgs boson cross section at next-to SV to NNLO + $\overline{\text{NNLL}}$, Eur. Phys. J. C **82**, 774 (2022).
[93] M. van Beekveld, E. Laenen, J. Sinninghe Damsté, and L. Vernazza, Next-to-leading power threshold corrections for finite order and resummed colour-singlet cross sections, J. High Energy Phys. 05 (2021) 114.
[94] A. A H, P. Mukherjee, and V. Ravindran, Going beyond soft plus virtual, Phys. Rev. D **105**, L091503 (2022).
[95] M. Beneke, M. Garny, S. Jaskiewicz, J. Strohm, R. Szafron, L. Vernazza, and J. Wang, Next-to-leading power endpoint factorization and resummation for off-diagonal "gluon" thrust, J. High Energy Phys. 07 (2022) 144.

[96] Z. L. Liu, M. Neubert, M. Schnubel, and X. Wang, Factorization at next-to-leading power and endpoint divergences in gg → h production, J. High Energy Phys. 06 (2023) 183.
[97] G. Sterman and W. Vogelsang, Power corrections to electroweak boson production from threshold resummation, Phys. Rev. D **107**, 014009 (2023).
[98] S. Pal and S. Seth, On Higgs + jet production at next-to-leading power accuracy, Phys. Rev. D **109**, 114018 (2024).
[99] M. C. Kumar, M. K. Mandal, and V. Ravindran, Associated production of Higgs boson with vector boson at threshold N^3LO in QCD, J. High Energy Phys. 03 (2015) 037.
[100] G. Das, C. Dey, M. C. Kumar, and K. Samanta, Threshold enhanced cross sections for colorless productions, Phys. Rev. D **107**, 034038 (2023).
[101] G. Das, C. Dey, M. C. Kumar, and K. Samanta, Precision studies for Higgs-Strahlung process at hadron collider, Springer Proc. Phys. **304**, 245 (2024).
[102] R. V. Harlander, A. Kulesza, V. Theeuwes, and T. Zirke, Soft gluon resummation for gluon-induced Higgs Strahlung, J. High Energy Phys. 11 (2014) 082.
[103] S. Moch, J. A. M. Vermaseren, and A. Vogt, The three loop splitting functions in QCD: The nonsinglet case, Nucl. Phys. **B688**, 101 (2004).
[104] A. Vogt, S. Moch, and J. A. M. Vermaseren, The three-loop splitting functions in QCD: The singlet case, Nucl. Phys. **B691**, 129 (2004).
[105] V. V. Sudakov, Vertex parts at very high-energies in quantum electrodynamics, Sov. Phys. JETP **3**, 65 (1956), http://www.jetp.ras.ru//cgi-bin/dn/e_003_01_0065.pdf.
[106] A. H. Mueller, On the asymptotic behavior of the Sudakov form-Factor, Phys. Rev. D **20**, 2037 (1979).
[107] J. C. Collins, Algorithm to compute corrections to the Sudakov form-factor, Phys. Rev. D **22**, 1478 (1980).
[108] A. Sen, Asymptotic behavior of the Sudakov form-factor in QCD, Phys. Rev. D **24**, 3281 (1981).
[109] A. A H, P. Mukherjee, V. Ravindran, A. Sankar, and S. Tiwari, Next-to SV resummed Drell–Yan cross section beyond leading-logarithm, Eur. Phys. J. C **82**, 234 (2022).
[110] M. van Beekveld, L. Vernazza, and C. D. White, Threshold resummation of new partonic channels at next-to-leading power, J. High Energy Phys. 12 (2021) 087.
[111] C. Anastasiou, C. Duhr, F. Dulat, F. Herzog, and B. Mistlberger, Higgs boson gluon-fusion production in QCD at three loops, Phys. Rev. Lett. **114**, 212001 (2015).
[112] B. Mistlberger, Higgs boson production at hadron colliders at N^3LO in QCD, J. High Energy Phys. 05 (2018) 028.
[113] C. Duhr, F. Dulat, and B. Mistlberger, Drell-Yan cross section to third order in the strong coupling constant, Phys. Rev. Lett. **125**, 172001 (2020).
[114] S. Catani, M. L. Mangano, P. Nason, and L. Trentadue, The resummation of soft gluons in hadronic collisions, Nucl. Phys. **B478**, 273 (1996).
[115] A. Vogt, Efficient evolution of unpolarized and polarized parton distributions with QCD-PEGASUS, Comput. Phys. Commun. **170**, 65 (2005).
[116] R. D. Ball *et al.* (PDF4LHC Working Group), The PDF4LHC21 combination of global PDF fits for the LHC Run III, J. Phys. G **49**, 080501 (2022).
[117] A. Buckley, J. Ferrando, S. Lloyd, K. Nordström, B. Page, M. Rüfenacht, M. Schönherr, and G. Watt, LHAPDF6: Parton density access in the LHC precision era, Eur. Phys. J. C **75**, 132 (2015).
[118] S. Navas *et al.* (Particle Data Group), Review of particle physics, Phys. Rev. D **110**, 030001 (2024).